

REVIEW



Cite this: *J. Mater. Chem. B*, 2017, 5, 2867

Received 30th January 2017,
Accepted 8th March 2017

DOI: 10.1039/c7tb00316a

rsc.li/materials-b

Covalently modified halloysite clay nanotubes: synthesis, properties, biological and medical applications

M. Massaro,^a G. Lazzara,^{*b} S. Milioto,^b R. Noto^a and S. Riela^{*a}

Halloysite (HNT) is a promising natural nanosized tubular clay mineral that has many important uses in different industrial fields. It is naturally occurring, biocompatible, and available in thousands of tons at low cost. As a consequence of a hollow cavity, HNT is mainly used as nanocontainer for the controlled release of several chemicals. Chemical modification of both surfaces (inner lumen and outer surface) is a strategy to tune the nanotube's properties. Specifically, chemical modification of HNT surfaces generates a nanoarchitecture with targeted affinity through outer surface functionalization and drug transport ability from functionalization of the nanotube lumen. The primary focus of this review is the research of modified halloysite nanotubes and their applications in biological and medical fields.

1 Introduction

Nanomaterials are defined as materials with at least one external dimension in the size range from approximately 1–100 nanometres. Until now, the behaviour of some nanomaterials like carbon

nanotubes, metal or metal oxide nanoparticles (e.g., gold, titanium dioxide), quantum dots, and many others is well understood, whereas others present greater challenges.

An emerging nanomaterial (Fig. 1), with appealing properties, is halloysite clay. The term 'halloysite', derived from Omalius d'Hallo, who found the mineral in Angleur Liège Belgium, was employed for the first time in 1826 by Berthier.¹

The beginning of the extensive research on halloysite as a mineral started in 1940 but only in the last 20 years it became available in pure form and it was utilized both as a "cylindrical mineral"² and as a "low-cost alternative nanotube".³

^a Dipartimento STEBICEF, Sez. Chimica, Università degli Studi di Palermo, Viale delle Scienze, Parco d'Orleans II, Ed. 17, 90128 Palermo, Italy.
E-mail: serena.riela@unipa.it

^b Dipartimento di Fisica e Chimica, Università degli Studi di Palermo, Viale delle Scienze, Parco d'Orleans II, Ed. 17, 90128 Palermo, Italy.
E-mail: giuseppe.lazzara@unipa.it



M. Massaro

Marina Massaro obtained her BSc (2009) and MSc (2013) degrees in Chemistry from the University of Palermo. In 2013 she spent three months at the University College of Dublin (Ireland) in the group of Dr Susan Quinn. In 2015 she received his PhD degree from the University of Palermo under the supervision of Prof. R. Noto and Dr S. Riela. Since 2015 she is Postdoc at the University of Palermo. Her current research

interests include the modification of halloysite nanotubes for application in several fields.



G. Lazzara

Giuseppe Lazzara received his PhD degree in Chemistry at the University of Palermo, Italy, in 2007. He was a Postdoc at the Chemistry Department, Lund University (Sweden). Lazzara became associate professor at the Department of Physics and Chemistry, the University of Palermo (Italy), in 2015. His research activities focus on smart nanomaterials, nanoparticles and polymer/nanoparticle interactions. He is involved in several projects

on halloysite clay nanotubes for drug delivery and conservation of Cultural Heritage. Lazzara has more than 85 publications in peer-reviewed international journals.

HNTs are natural nanomaterials with a unique combination of a hollow tubular nanostructure, large aspect ratio, mechanical strength, broad potential in terms of functionality, biocompatibility, and availability in large amounts at low cost. In addition, halloysite is proven to be a bio- and eco-compatible material as shown by several *in vitro* and *in vivo* studies.^{4–11}

Finally, HNTs are among the few nanotubes with a different composition of inner and outer surfaces that allow for different modification methods by simultaneous immobilization of two or more functional groups. Since 2008, the modifications of halloysite surfaces opened up the use of these nanomaterials for several applications in many fields. The main focus of this review is the research of covalently modified halloysite

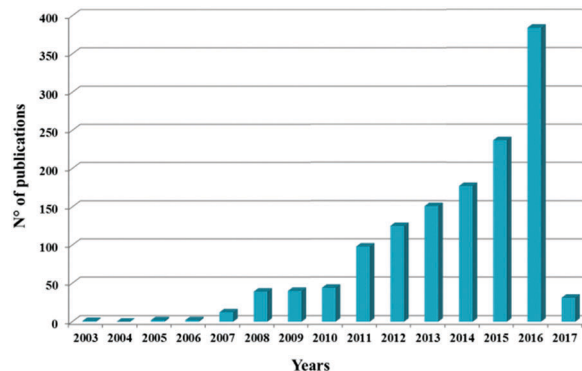


Fig. 1 Comparison of the annual number of scientific publications on the "halloysite nanotubes" term in the past 20 years. (Data analysis of publications was done using the SciFinder Scholar search system with the term "halloysite nanotubes", as on December 2016).



S. Milioto

Stefana Milioto received her Master Degree in Chemistry at the University of Palermo in 1985. She defended her PhD thesis in Chemical Sciences in 1989. Then she was a Research Scientist (until 1998) and Associate Professor (until 2001) in Physical Chemistry. At present she is Full Professor in Physical Chemistry at the Department of Physics and Chemistry of the University of Palermo. Her scientific interest deals with the

physicochemical studies of eco-compatible nanostructures (self-assembled structures as well as solid nanoparticles) functionalized for application in the field of Cultural Heritage, drug delivery, and so on. She has more than 125 publications in peer-reviewed international journals.

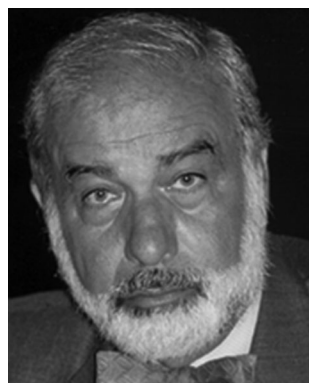
nanotubes and their biological and medicinal applications that have been detailed in the literature.

2 Characteristics of halloysite

2.1 Structure

Halloysite (HNT) has a chemical formula for its cell unit $\text{Al}_2\text{Si}_2\text{O}_5(\text{OH})_4 \cdot n\text{H}_2\text{O}$ that corresponds to kaolinite, a natural aluminosilicate clay. It is a dioctahedral 1:1 clay mineral present in soils. It is formed by weathering of several types of igneous and non-igneous rocks, and thus it can be found mainly in wet tropical and subtropical regions and weathered rocks. Of course, each deposit is characterized by different purity grades, characteristic sizes and hydration states.

The layer unit consists of a corner-shared tetrahedral SiO_4 sheet stacked with an edge-shared octahedral AlO_6 sheet with an internal aluminol group $\text{Al}-\text{OH}$. When $n = 2$ the mineral is



R. Noto

Renato Noto obtained his chemistry degree from the University of Palermo in 1970. He has been Full Professor of Organic Chemistry since 1990. He began his research activity in the field of physical organic chemistry. Then his interest moved to the stereo-controlled synthesis of functionalized heterocyclic rings and to studies on inclusion equilibria of aromatic molecules in cyclodextrins. Recently he has addressed his attention to the

behavior of organic salts as ionic liquids and/or gelators and to use of functionalized halloysite nanotubes as catalytic systems or drug carrier systems. He is the author of more than 200 publications and five reviews.



S. Riela

Serena Riela since 2002 is an Assistant Professor at the University of Palermo. She received her PhD from the University of Bologna in 2000, under the supervision of Prof. D. Spinelli. From April 2001, she was a post-doctoral researcher at the Organic Chemistry Department of the University of Palermo. She spent one year at the University of California Los Angeles (UCLA) under the supervision of Prof. J. F. Stoddart and eight months at the

University of Bordeaux 1 under the supervision of Prof. A. Castellan. Her current interests are focused on the chemical modification of halloysite nanotubes and their applications in catalysis, drug delivery, bioremediation and so on. Riela is the author of about 60 publications in peer-reviewed international journals.

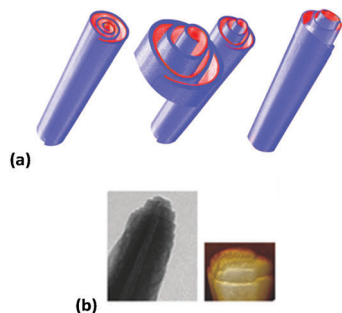


Fig. 2 (a) Schematic representation of the rolled structure of halloysite; (b) TEM and AFM images of HNT edges.

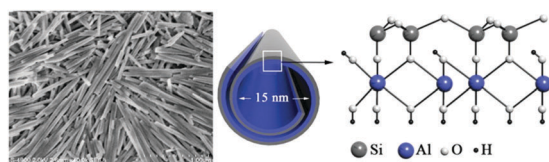


Fig. 3 FE-SEM image of halloysite on Si-wafer (left) and schematic illustration of the crystalline structure of halloysite (right). Reproduced from ref. 18 with permission from The American Chemical Society.

called halloysite-10 Å due to its layer periodicity of 10 Å, whereas heating halloysite-10 Å to 120 °C irreversibly dehydrates it to halloysite-7 Å with $n = 0$.¹²

How halloysite nanotubes are formed is still under debate.¹³ There are few papers that report, from a theoretical point of view, halloysite modelling to obtain information about the tubular structure of this clay.

A first attempt to model halloysite nanotubes was made by Guimaraes *et al.*,¹⁴ more recently, Ferrante *et al.* reported,¹⁵ for the first time, the molecular *ab initio* calculations on spiral halloysite nanotubes, both in the hydrated form and in the anhydrous form. The authors found that, in the hydrated HNT form, the water molecules should have a major effect on stabilizing the spiral structure compared to the unrolled one.

HNT has mainly a hollow tubular structure in the sub-nanometre range with an aspect ratio of *ca.* 20; the wall is constituted of 10–15 bilayers of aluminum and silicon oxide (Fig. 2). Depending on the deposit the halloysite dimensions can vary. Generally HNTs have a length in the range of 0.2–1.5 μm, while the inner and outer diameters of the tubes are in the ranges of 10–30 nm and 40–70 nm, respectively^{12,16,17} (Fig. 3).

2.2 Physicochemical properties

The techniques typically used to characterize HNT nano-materials are: FTIR spectroscopy,¹⁹ used to analyze the outer and inner active molecule loading, as well as UV-vis or fluorescence spectroscopy; SEM and TEM to image the tubular structure;²⁰ thermogravimetric analysis (TGA);²¹ ζ potential, pH, specific surface area and pore volume used to determine the specific interaction with suitable molecules.

The dielectric properties of aluminum and silicon oxides are different. Similarly, they undergo ionization in aqueous media

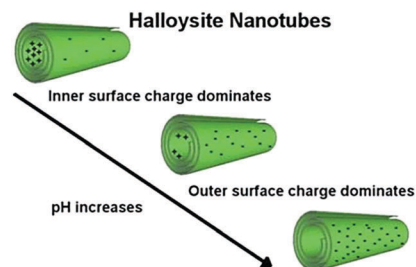


Fig. 4 Charge separation between the inner and outer surfaces of HNT. Reproduced from ref. 23 with permission from The American Chemical Society.

in an opposite way generating tubes with inner and outer surfaces oppositely charged. This charge separation occurs in water within a wide pH range from 3 to 8.²² Experimentally, the charge separation is predicted by comparing the negative and positive values for electrical ζ-potential of silica and alumina surfaces in water, respectively (Fig. 4). Therefore, the outermost layer of the halloysite tubes containing silica possesses an electrical ζ-potential of *ca.* −30 mV in the pH range mentioned above. This nanotube surface charge halloysite contributes to moderate colloidal stability in water (2–3 h). The superimposition of the negative silica outermost surface with the positive (alumina) inner lumen results in the fact that the measured ζ-potential of HNTs is less than that of pure silica particles (−50 mV).

This charge separation is strictly dependent on the acid–base properties of HNTs. To understand the aqueous behavior of these peculiar nanotubes Pettignano *et al.*²³ studied the protonation/deprotonation equilibria of Si–OH and Al–OH groups by a ISE-H⁺ potentiometric titration under variable pH, ionic strength, ionic medium and concentration conditions (Fig. 4). In particular, one protonation constant for the Si–OH groups and two for the Al–OH groups were determined. The protonation constant values increase with increasing ionic strength in all ionic media, suggesting the presence of a background electrolyte which stabilizes the protonated species through the formation of weak complexes between ions of the supporting electrolytes and the protonated species (Fig. 5).

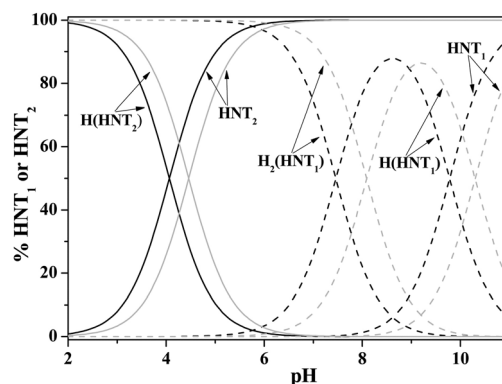


Fig. 5 Distribution diagrams of the HNT1 (dashed lines) and HNT2 (continuous lines) protonated and weak complex species vs. pH in NaCl, at $I = 0.100 \text{ mol dm}^{-3}$. Experimental conditions: $C_{\text{HNT1}} = 1 \text{ mmol dm}^{-3}$, $C_{\text{HNT2}} = 4 \text{ mmol dm}^{-3}$, $T = 298.15 \text{ K}$. Reproduced from ref. 23 with permission from The American Chemical Society.

2.3 Halloysite biocompatibility

The increasing interest in HNT nanomaterials could result, in the long term, in the release and accumulation of the nanoclay in the environment with consequential damage to human health and/or vegetation.

The first example of the phytotoxic study on halloysite was reported by Riela and Scialabba *et al.*,⁹ who performed experiments on *Raphanus sativus* L to develop a quantitative risk assessment model for predicting the potential impact of HNT on plant life.

Halloysite is proven to be a biocompatible material in several recent reports on cell cultures²⁴ and invertebrate models.⁷ The uptake and toxic effects of halloysite have been investigated using human cell lines, namely breast cancer cells,²⁴ thyroid cancer cells,^{25–27} hepatic cancer cells^{28,29} and epithelial adenocarcinoma cells.²⁴ The toxicity of HNT was tested after 48 hours of incubation with fibroblast and human breast cells.²⁴ It emerged that it is non-toxic and it is much less harmful than ordinary sodium chloride salt. The introduction of a functionality on the HNT surface could, in principle, induce some adverse effects. For example, chitosan scaffolds for tissue engineering doped with halloysite were found to induce no significant adverse effects on the attachment and development of fibroblasts. Composite halloysite-doped dental scaffolds stimulated the growth of fibroblast cells.³⁰ In contrast, the functionalization of HNT with organic groups that themselves possess biological activities, such as triazolium salts, confers an antiproliferative activity to halloysite.^{25,29}

The interaction of halloysite nanotubes with microscopic algae *Chlorella pyrenoidosa* was also investigated. Lvov *et al.*³¹ demonstrated that there was no penetration of the nanomaterials into the cell interior. It was also reported that halloysite nanotubes were safe for one of the most common fresh water ciliate protists *Paramecium caudatum*.⁴ Similarly, HNTs exhibit no toxicity towards *Escherichia coli* bacteria³² and yeast cells.³³

Fahrkrullin *et al.*⁷ reported the first example of the evaluation of halloysite toxicity *in vivo* on free living nematodes (worms) *Caenorhabditis elegans*. The authors demonstrated that HNTs were found exclusively in the intestines of the worms and no nanotubes were detected outside the intestines of the nematodes (Fig. 6).

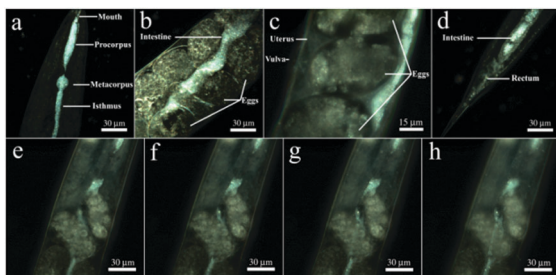


Fig. 6 Dark-field microscopy imaging of distribution of halloysite in *C. elegans* worms: (a) inside the foregut; (b and c) in the midgut (no nanotubes in embryos, uterus, and vulva were detected); (d) inside the hindgut. (below) *In vivo* effects on *C. elegans* growth and fertility. Reproduced from ref. 37 with permission from The Royal Society of Chemistry.

Therefore, halloysite within a wide range of concentrations does not damage the organism of the nematodes, inflicting only mechanical stress on the alimentary system. Halloysite is efficiently removed from an organism by macrophages and therefore it is considered a healthy and biocompatible material, though it may penetrate into the cell interior as shown by confocal microscopy experiments.²⁴ It turned out that accumulation of HNTs within cells does not prevent their proliferation and they are taken up into the cells surrounding the nuclei. The introduction of targeting moieties on halloysite involves an accumulation of halloysite into the cell, with specific interaction with cell nuclei, as confirmed by fluorescence microscopy. The specific functionalization of HNT with sugar moieties (HNT-CD) generates a high propensity to cross cell membranes, penetrating into the cell nucleus (Fig. 7).²⁷ However, because there are not biological mechanisms of aluminosilicate degradation in the body, halloysite is not biodegradable, and therefore it cannot be injected intravenously. The use of modified halloysite is limited as an active ingredient in external medical treatment with slow release of encapsulated drugs (*e.g.*, in creams, implants, or wound treatment of tissues). Several studies were performed in order to assess the cytotoxicity of HNT for the potential of oral dosage. In particular Shaib *et al.*³⁴ studied, by means of WST-1 assay, the effect of the nanomaterial on two cell lines, namely the colorectal carcinoma cells HCT116 and the hepatocarcinoma cells HepG2. In addition, the authors studied the cytogenetic toxicity of HNT by determining its activity against human peripheral lymphocytes by means of the mitotic index assay. The obtained results highlighted that halloysite nanotubes are safe materials and they can be used in various oral drug delivery systems, particularly as diluents/filler materials in tablets, capsules, and suspensions, without causing toxicity to the absorptive sites and the first accumulating organ. In this context, HNTs were used as tablet excipients with excellent compression properties for the delivery and controlled-release of nifedipine. This formulation ensured a sustained release up to 20 hours of the active agent and protected it from photo-degradation.³⁵

Finally, Mitrokhin *et al.* recently demonstrated that halloysite can be classified as a hazard class 4 material (low hazard substance).³⁶

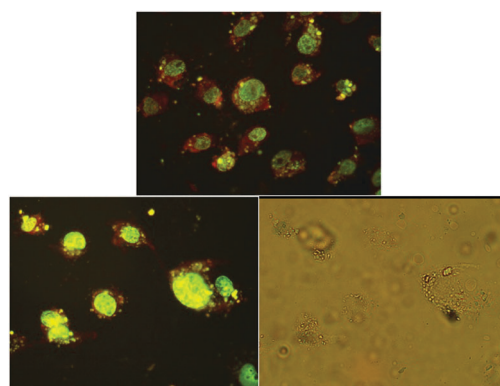


Fig. 7 Fluorescence microscopy images of the HNT-CD uptake by 8505C. The 8505C cell membrane (red) with co-localized HNT-CD (green) inside nuclei at 24 h.²⁷

3 Modification of halloysite

Among the different phyllosilicate nanomaterials (silicate based layer structure) such as kaolin and montmorillonite, halloysite has distinct advantages. First of all it is composed of small tubes that, compared to other tubular nanomaterials, have dimensions that allow for macrophage removal of nanoparticles from a living organism.¹² In addition the empty HNT lumen can be loaded with active molecules (drugs) or alternatively, drugs can be absorbed onto the external HNT surface.

Furthermore, the possibility of both loading the drug into the inner lumen and grafting it onto the outer surface offers distinctive additional advantages, *i.e.* synergism between drugs with different biological properties.

The remaining sections are focused on the introduction of chemical modifications on the HNT external surface and the simultaneous supramolecular interactions of drugs with the HNT lumen.

The most attractive feature of halloysite is its inner lumen with a diameter capable of entrapping chemical agents such as macromolecules, drugs, DNA, proteins, nanodots³⁸ and other chemically active agents, *e.g.*, anticorrosion for protective coating. In this context, the empty lumen of halloysite acts as a miniature container for processes, which benefit from sustained molecular release.

The use of halloysite as a nano-container for drug loading and release was firstly introduced by Price, Gaber and Lvov, who used the nanotube as a carrier for oxytetracycline HCl (a water soluble antibiotic); khellin (a lipophilic vasodilator) and nicotinamide adenine dinucleotide (NAD) (an important co-enzyme).² Successively, Veerabadran *et al.*²² reported that halloysite can load and release dexamethasone and furosemide in a controlled manner.

Electrostatic interactions were used to selectively load, into the positively/negatively charged HNT lumen/outer surface, protein with diameters of 3–8 nm; in particular, the immobilization of laccase, glucose oxidase, lipase, and pepsin was reported.³⁹

To avoid the fast release of the active agent from the HNT lumen, Fakhrullin *et al.*⁴⁰ fabricated a novel drug delivery system based on HNTs loaded with brilliant green as a drug model, and coated with dextrin to clog the tube opening until the cell absorbs these nanocarriers whereupon the sugar can be cleavable by intercellular glycosyl hydrolases (Fig. 8). They found that the accumulation and enzymatically induced release

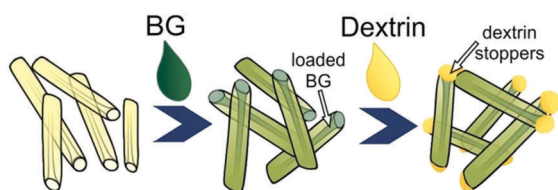


Fig. 8 Fabrication of brilliant green-loaded HNTs and the subsequent coating with dextrin stoppers. Reproduced from ref. 40 with permission from the Nature Publishing Group.

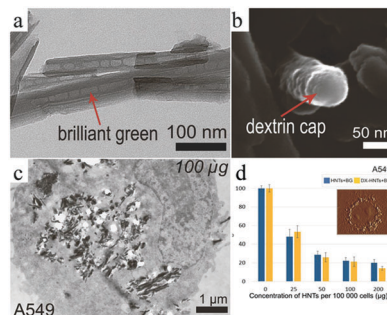


Fig. 9 (a) TEM image of brilliant-green-loaded halloysite; (b) SEM image of a dextrin cap at the end of the functionalized nanotube; (c) TEM images of A549 cells incubated with dextran-coated clay nanotubes; (d) resazurin assay results demonstrating the LD₅₀ value of BG-loaded halloysite for A549 cells. The insets show the AFM images of the distribution of DX-halloysite in the A549 cells. Reproduced from ref. 40 with permission from the Nature Publishing Group.

of drugs occurred exclusively in cells prone to internalization of the nanotubes with higher proliferation rates, which is a characteristic of tumoral cells. Therefore, the developed nanomaterial does not damage healthy cells and as a result, drug-loaded dextrin-HNTs will be accumulated selectively in tumor cells (Fig. 9).

However, pristine halloysite shows only weak interactions with guest molecules through hydrogen bonding or van der Waals forces,⁴¹ and fast and non-controlled release.⁴² Therefore, it is clear that the functionalization of halloysite surfaces is crucial to solve the aforementioned drawbacks. Fortunately, the different inside/outside halloysite chemistry allows for selective functionalization of the surfaces, which increases the potential applications of HNT.⁴³ The covalent modification of the outer surface is most commonly achieved by grafting silanes *via* condensation between hydrolyzed silanes and the surface hydroxyl groups of the HNTs located on the edges or on external surface defects.³⁷

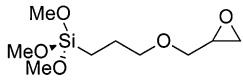
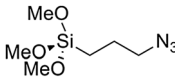
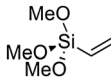
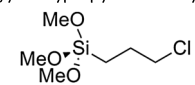
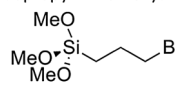
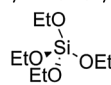
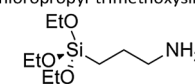
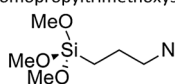
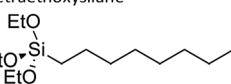
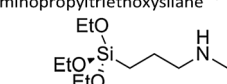
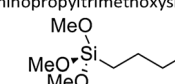
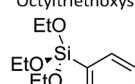
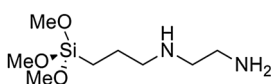
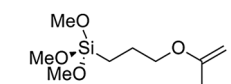
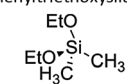
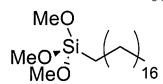
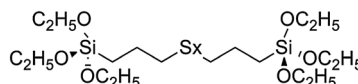
The grafting reactions can occur in toluene, in water/alcohol mixtures or under solvent-free conditions under microwave irradiation. Over the years, numerous silanes have been grafted onto HNTs with the aim of preparing nanomaterials with hierarchical nanostructures (Table 1).

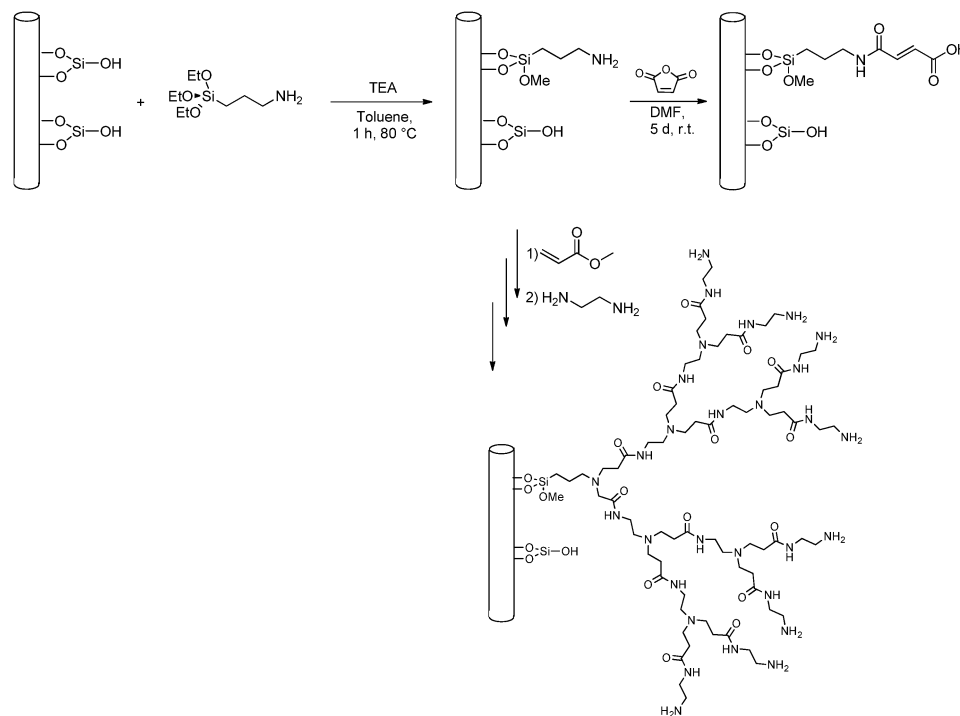
For example, the modification of the halloysite nanotubes by γ -methacryloxypropyl trimethoxysilane increases the interactions with the ethylene propylene diene monomer and the degree of dispersion of the HNTs in the polymeric matrix.⁴⁴

Once a specific organosilane is grafted onto the HNT external surface, it is possible to introduce other functionalities by modifying the organosilane terminal group. For example, it is possible to obtain a HNT-COOH nanomaterial by reacting the amino functionality of a APTES functionalized HNT with maleic or succinic anhydride in DMF (Fig. 10).^{45–47}

In another work, amine-terminated dendritic groups were attached on the surface of HNTs by a divergent synthesis starting from HNT-APTES and methyl methacrylate (MA) as monomers, followed by reaction with ethylene diamine to obtain a third generation dendrimer functionalized halloysite (Fig. 10).⁴⁸

Table 1 The chemical composition of silanes used for the modification of HNTs

		
γ -glycidoxypropyltrimethoxysilane ^{51, 52}	3-azidopropyltrimethoxysilane ²⁵	Vinyltrimethoxysilane ^{53, 54}
		
3-chloropropyl-trimethoxysilane ⁵⁵	3-bromopropyltrimethoxysilane ⁵⁴	Tetraethoxysilane ⁵⁶
		
3-aminopropyltriethoxysilane ^{37, 42, 57}	3-aminopropyltrimethoxysilane ⁵⁸⁻⁶⁰	Octyltriethoxysilane ^{56, 61}
		
[3-(methylamino)propyl]trimethoxysilane ⁶²	3-mercaptopropyltrimethoxysilane ^{63, 64}	Phenyltriethoxysilane ⁵⁴
		
[3-(2-aminoethylamino)propyl]trimethoxysilane ^{18, 32, 54, 65, 66}	3-(trimethoxysilyl)propyl methacrylate ^{44, 67, 68}	Diethoxy diethylsilane ⁶⁹
		
Trimethoxy(octadecyl)silane ⁶¹		Bis-[3-(triethoxysilyl)propyl] tetrasulfide ⁶⁹

**Fig. 10** Examples of further functionalization of APTES modified HNT.

The HNT-NH₂ scaffolds were also used as precursors for polymer attachment on the HNT external surface. Several polymers have been covalently grafted by means of simple condensation reactions, such as polyethyleneimine⁴⁹ or poly *N*-isopropyl acryl amide.⁵⁰

4 Application of modified HNTs as drug carrier and delivery systems

The applications of HNT nanomaterials are expected to increase as a consequence of the modification of halloysite surfaces,

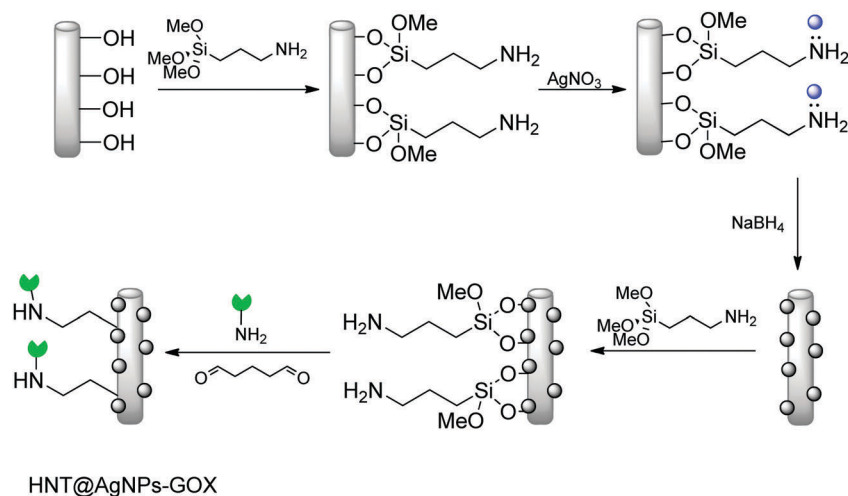


Fig. 11 Schematic illustration of the selective modification of the HNTs and subsequent grafting of AgNPs and site-specific covalent immobilization of the GOx enzymes.

which opens up alternative ways to the use of nanoclay, in particular in the field of drug delivery.

The advantage of using a halloysite as a nanocontainer for active molecules lies in the benefit of their sustained release over time. Compared to the compound dissolved in water, the molecules interacting with HNT exhibit much longer release rates, indicating nanopore controlled diffusion from HNT. Usually, release rates increase from few minutes to 20 h in the presence of HNT. For example, nicotinamide adenine dinucleotide (NAD) was released in 5 h while dexamethasone release takes place in 10–15 h, where only 60% of the drug was released in the first 6 h. In addition, the possibility of introducing HNT as a filler in polymeric or hydrogel matrices further slows the release rate of a given compound.

Veerabadrán *et al.*⁷⁰ elaborated a layer by layer assembly (LbL) by sequentially absorbing layers of polyelectrolytes of different molecular weights, with a final layer of silica nanoparticles. LbL shell assembly was applied to dexamethasone loaded halloysite to slow the drug release from the nanotubes. The loading of the drug was confirmed by porosity measurements that showed a reduction in the pore volume of the dexamethasone loaded HNT compared to the unloaded tube. The drug loading was estimated, by UV experiments, to be *ca.* 7 vol%, which is approximately the lumen volume.

The covalent functionalization of the external surface of halloysite with 3-aminopropyltriethoxysilane (APTES) improved ibuprofen (IBU) loading by creating an electrostatic attraction between the introduced aminopropyl groups of the grafted APTES and the carboxyl groups of IBU. The electrostatic attraction was stronger than the hydrogen bonding in the case of IBU loading in unmodified halloysite.⁷¹ The release of IBU from the APTES-modified and pristine HNT fits with the modified Korsmeyer–Peppas model.[†] The strong affinity

[†] $F_t = kt^n$, where F_t is the drug release fraction at time t , k is the kinetic release constant, t is the release time and n is the characteristic diffusion exponent, depending on the release mechanism and the geometry of device. If Fickian diffusion occurred, n decreased to 0.5 for slab/cylinder/sphere. If non-Fickian (anomalous) diffusion dominated, the n value was between the above value corresponding to the polymer chain relaxation ($n < 1$) for a slab/cylinder/sphere. Thus, through determination of the n value, the drug release mechanism could be identified.

(electrostatic attraction) in APTES-modified HNT slowed the release of IBU and changed the release mechanism from Fickian diffusion in the pristine HNT to non-Fickian diffusion in the APTES-HNT.⁴²

The performance of HNT functionalized by APTES was also studied for the loading and release of aspirin.⁵⁷ The results obtained show that the introduction of APTES on the HNT surface improved the drug loading from 3.84 to 11.98 wt% with respect to pristine halloysite. In addition, the obtained hybrid significantly enhances the dissolution rate of the drug by creating a burst release with the first hour followed by sustained release for *ca.* 16 hours compared with the free aspirin. Furthermore, if compared with drug release from pristine halloysite, the aspirin dissolution rate from the modified HNT is slower.

A similar system was used by Kumar-Krishnan *et al.* to obtain a novel nanomaterial able to immobilize efficiently, after AgNP coating, enzyme glucose oxidase (GOx) (Fig. 11).⁷² The immobilization of GOx is crucial since the direct physical adsorption of enzymes over the solid matrix often leads to partial deactivation of their biocatalytic functions and consequently direct electron transfer is not observed.⁷³ Similarly, the immobilization of enzymes over 3D redox polymer matrices significantly impacts the charge-transfer efficiency. The modification of HNT improves the GOx immobilization but also revealed a high electrocatalytic activity for glucose reduction and facilitating enhanced charge transport. The glucose detection sensitivity of the composite electrodes was as high as 5.1 $\mu\text{A mM}^{-1} \text{cm}^{-2}$, which is considerably higher than the glucose sensitivity of the electrode fabricated by a non-functionalized HNT/AgNP surface. The modification of the halloysite surface with succinic anhydride, as mentioned in the Introduction, is a useful tool to convert the surface hydroxyl groups to carboxyl groups creating a suitable scaffold available for further functionalization. The so-obtained HNTs-COOH was connected to biocompatible chitosan *via* *N*-(3-dimethylamino-propyl)-*N'*-ethylcarbodiimide/*N*-hydroxysuccinimide reaction, forming the HNTs-*g*-chitosan hybrid.⁴⁵ Afterwards, curcumin was loaded onto the surface of HNTs-*g*-chitosan through supramolecular interactions. The covalent grafting of chitosan on HNTs

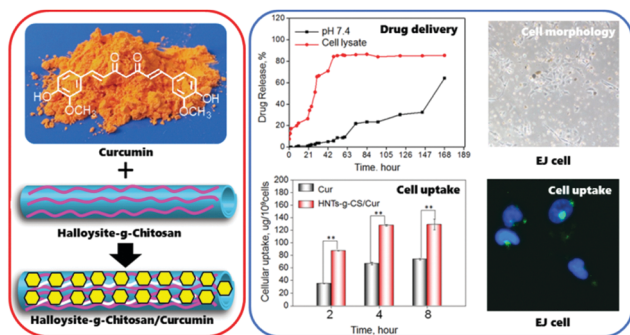


Fig. 12 Curcumin loaded on the HNTs-g-chitosan hybrid. Reproduced from ref. 45 with permission from The Royal Society of Chemistry.

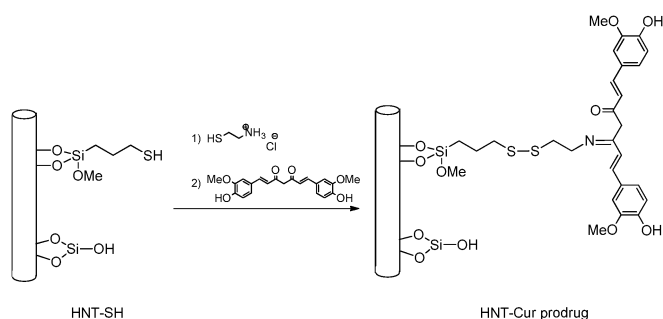
increases the hemocompatibility, stability in body liquid, the loading efficiency of curcumin, and the cytocompatibility (Fig. 12). HNTs-g-chitosan acts as a highly potent killer of various cancer cells *in vitro* especially with higher cytotoxicity to EJ human bladder cancer cells compared to free curcumin from the cell viability assay. In addition, the supramolecular hybrid HNTs-g-chitosan/curcumin was successfully taken up by cancer cells, as confirmed by fluorescence microscopy.

In recent work,⁷⁴ the same authors reported the application of the HNT-g-chitosan system as carrier for doxorubicin (Doxo). They found that the system is highly efficient in the drug loading preserving Doxo properties. Furthermore, release tests show a controllable and sustained release in the “tumoral environment” instead of under normal physiological conditions. Doxo release from the HNT-g-chitosan system was, indeed, very slow in PBS solution (only 6.40% was released after 45 h), while it was fast in the cell lysate, where 61.9% of release was observed after 12 h.

4.1 Prodrugs based on HNT

The first attempt to obtain a HNT based prodrug reports the curcumin covalently linked on the halloysite external surface through GSH- or pH-responsive bonds (HNT-Cur prodrug) (Scheme 1).²⁸

The morphology and the size of the HNT prodrug were characterized by SEM and dynamic light scattering (DLS). Measurements of the particle size using DLS revealed an apparent hydrodynamic radius of 570 nm for the HNT-Cur prodrug.



Scheme 1 Schematic representation of the synthesis of the HNT-Cur prodrug.

This value is *ca.* 2 times larger than that expected for a single diffusive HNT particle (240 nm).⁷⁵ The outer surface modification with Cur is expected to enhance the hydrophobic lateral interaction between nanotubes. The formation of supramolecular aggregates is therefore evidenced by slow diffusion or hydrodynamic radius increase.

On the other hand, SEM images of the dried samples show that the tubular morphology is preserved in the HNT-Cur prodrug as well as the characteristic sizes of the imaged nanotubes that are 80 nm and 720 nm for the average external radius and length, respectively.

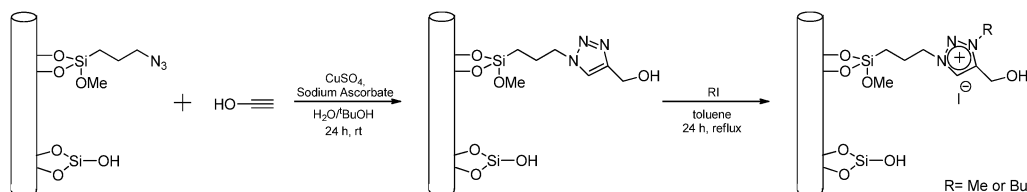
The halloysite prodrug showed relatively good stability under normal physiological conditions, and as a consequence of the dual stimuli-responsive nature of this nanomaterial, enhanced release of curcumin was observed upon exposure of the prodrug to GSH-rich or acidic conditions similar to the cellular microenvironment of hepatic cancer cells.

The release of curcumin from the HNT-prodrug was fitted with the Korsmeyer-Peppas model.[†] The results showed that the value of kinetic constant in an acidic environment was lower than 96% with respect to that at pH 7.4. This result indicates that different release mechanisms occur as a function of pH, in particular, a fast diffusion mechanism of curcumin ($k = 14 \pm 1 \text{ min}^{-1}$, $n = 0.08$) through the dialysis membrane at pH 7.4 as a consequence of the instantaneous disulphide bond reduction by GSH. In contrast, the HNT-Cur prodrug exhibits a sustained-release feature ($k = 0.6 \pm 0.2 \text{ min}^{-1}$, $n = 0.6$) at pH 1 in agreement with the hydrolysis of the imine bond.

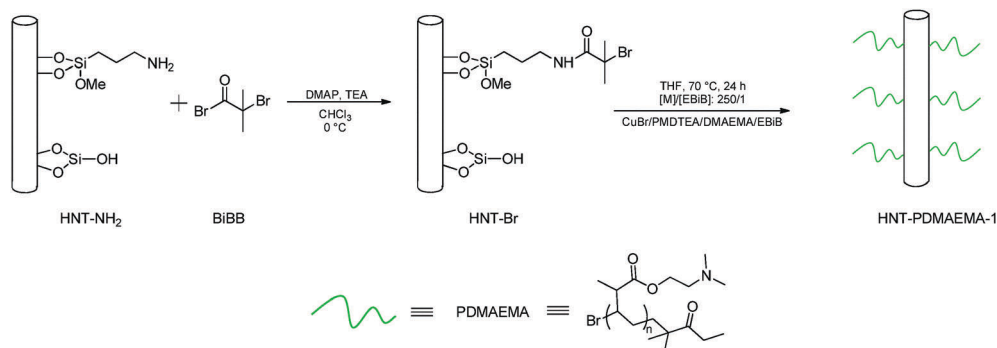
The antiproliferative *in vitro* studies on two cell lines of hepatocellular carcinoma showed that the HNT-Cur prodrug induced high cytotoxicity with respect to the free curcumin or pristine HNT. The opportunity to increase the release of curcumin from the nanoparticle by intracellular GSH appears very interesting, especially for hepatocarcinoma, because GSH is typically concentrated in hepatic cells. Furthermore, it was demonstrated that the HNT-Cur prodrug retains its antioxidant characteristics that could be crucial in anticancer therapy.

Another prodrug system based on halloysite was obtained by the functionalization of the HNT external surface with triazole molecules.

Triazoles and their derivatives, indeed, occupy a central position among the most significant compounds that constitute pharmaceutically and medicinally important drug centers.⁷⁶ Several triazoles have been reported to possess antifungal, antibacterial and antitumoral activities.²⁵ For the above reasons halloysite was firstly modified with 3-azidopropyl-trimethoxysilane and the nanomaterial obtained was used as a scaffold for the covalent grafting of triazolium ionic liquids (Scheme 2) to obtain a HNT-triazolium prodrug. The cytotoxicity of the new nanomaterial obtained was tested, by the MTT or MTS assay, against different tumoral cell lines, namely 8505C, BCPAP, C643, SW1736, HA22T/VGH, Hep3B and HepG2. It was found that the introduction of triazole moieties on halloysite involves an increase in the cytotoxicity of the HNT-triazolium prodrug with respect to pristine HNT with an IC_{50} of $40.0 \pm 14.6 \text{ mM}$.²⁵



Scheme 2 Schematic representation of the synthesis of the triazolium salt modified HNT.



Scheme 3 Schematic representation of the functionalization of HNT-NH₂ with BiBB and subsequent grafting of PDMAEMA chains.

4.2 Stimuli-responsive carriers

As far as the drug delivery issue is concerned, the development of a system that responds to a specific stimulus for the triggered release of the active component is often requested. The main advantage of this kind of stimuli-responsive prodrug is the reduction of side effects and the increase of antitumor activity owing to tumor-specific drug release.

Stimuli responsive polymers are a class of compounds that show conformational changes upon an external stimulus such as temperature, light, pH, and so on. Therefore, covering the halloysite surface with these types of polymers could generate novel materials with lots of potential applications in the fields of scaffolds for tissue engineering, biosensors and drug delivery systems.

4.2.1 pH-Sensitive delivery. Among the diversity of polymers that can be used for this purpose, pH-sensitive polymers have been attracted a lot of interest for their application in medicine. Poly(*N,N*-dimethylaminoethyl methacrylate) (PDMAEMA) is a pH-responsive polymer that possesses specific biological properties such as antibacterial properties and biocompatibility. For the above mentioned reasons HNTs were functionalized with PDMAEMA and used as drug delivery systems for diphenhydramine hydrochloride and diclofenac sodium salt (Scheme 3).⁷⁷ HNT was functionalized with APTES by the classic silane coupling reaction. Then, α -bromoisobutyryl bromide (BiBB) was anchored to the amine groups by an acylation reaction to yield HNT-Br and, finally, initiator-anchored HNT was used as a precursor to attach PDMAEMA onto the HNT external surface (Scheme 3). The so obtained nanomaterial was employed for DPH and DS loading, and the *in vitro* release of drugs was studied under different pH conditions. The DPH or DS release rate from the HNT-PDMAEMA was much slower than the release rate from pristine HNT (fast). This result is due to the polymer chains on the HNT surface

that exert a slowing effect on the release of drugs. Indeed, the movement of drug molecules from the inner space toward the lumen is hindered by the polymer chains and results in a low release rate. It was also found that the release of drug molecules from the nanomaterial is highly dependent on pH (Fig. 13). Indeed, in acidic medium, amine groups of PDMAEMA chains are protonated and formed a positively charged polyelectrolyte. The repulsion between the protonated PDMAEMA chains grafted on HNT resulted in a stretched chain conformation. This also affected the release behavior of HNT-PDMAEMA upon increasing the release rate of trapped DPH molecules among the polymer chains. Moreover, repulsions between the DPH molecules and protonated PDMAEMA chains accelerate the release of drug molecules.

4.2.2 Thermo-responsive carriers. Another stimuli-responsive carrier, in particular a thermo-responsive system, was obtained by introducing on the halloysite surface a thermo-responsive

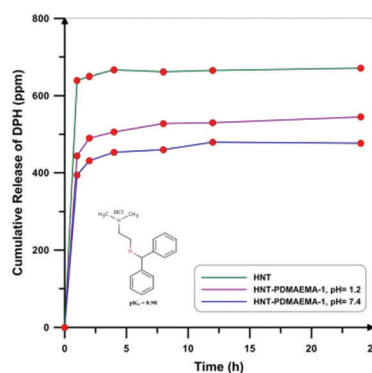


Fig. 13 Cumulative release of DPH from HNT and HNT-PDMAEMA-1 at two different pH values. Reproduced from ref. 77 with permission from Elsevier.

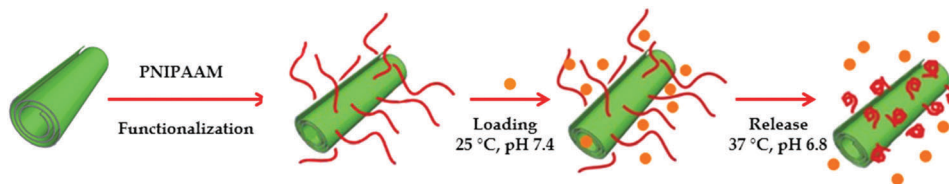


Fig. 14 Schematic representation of temperature triggered loading and release of curcumin into HNT modified with poly(*N*-isopropylacrylamide).

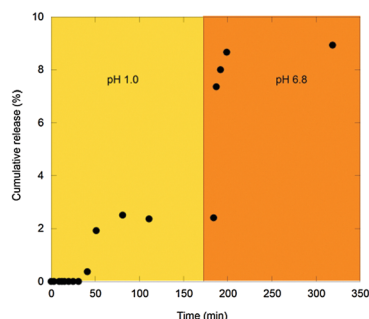


Fig. 15 Cumulative release of curcumin from HNT-PNIPAAm at pH 1.0 and pH 6.8.

polymer such as poly-*N*-isopropyl acrylamide (PNIPAAm).⁵⁰ This polymer was attached, by amide condensation, on the external HNT surface previously modified with 3-aminopropyl-trimethoxysilane (Fig. 14). The synthetic route adopted in this work rendered a large surface density of polymers onto the nanotubes. Temperature-responsive features were observed as the PNIPAAm corona undergoes a coil-to-globule transition at the lower critical solution temperature (LCST), around 32 °C. This material was used for curcumin delivery; the drug was loaded onto the carrier at 25 °C, whereas the drug release was investigated at 37 °C in a medium that simulates the gastro-intestinal transit (Fig. 15). The *in vitro* release tests showed a targeted and sustained release of the active species into the intestine.

5 Dual drug co-delivery

A novel dual drug co-delivery system was proposed by Lazzara and Riela *et al.* by the loading of curcumin or cardanol on the HNT-triazolium prodrug.^{25,29}

The successful loading was confirmed by several techniques. In particular, with regard to curcumin loading, TGA data showed the co-existence of two kinds of curcumin species, one encapsulated in the inner lumen, and the other adsorbed on the external surface (Fig. 16).^{75,78}

With regard to cardanol, HPLC analysis highlighted the strong interaction occurring in HNT-triazolium prodrug/Card supramolecular complexes.

In comparison with pristine HNT, these systems have the advantage of high drug encapsulation efficiency as well as pH-controlled and sustained release capabilities. Moreover, the triazole moiety on the HNT external surface was found to have a synergic effect with curcumin or cardanol, which makes the

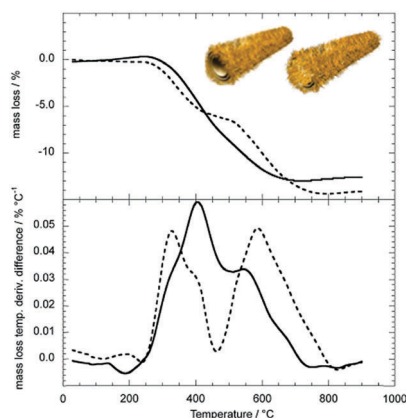


Fig. 16 TGA data revealed the co-existence of two different curcumin species loaded on HNT.

functionalized HNT an ideal carrier for anti-cancer therapies as confirmed by MTT and MTS assays on several tumoral cell lines.

The covalent linkage of a given drug on a suitable matrix is an important task in the development of new drug delivery systems since, besides the possibility of introducing a stimuli-responsive behavior, it is expected to minimize the undesired leaching of the drugs during circulation in the human body. Based on the above considerations, the halloysite surface was covalently functionalized with an antioxidant molecule, such as Trolox, that could benefit from a covalent linkage owing to a reduction in their toxicity by decreasing their steady-state concentration in the system. The first example of a synergic nanoantioxidant was based on Trolox covalently linked on the external surface of halloysite and quercetin loaded into the HNT lumen (Fig. 17a).⁷⁹ This novel nanomaterial represents the prototype for a general design strategy expected to afford improved antioxidant halloysite nanotubes, in which one main phenolic antioxidant function (like Trolox) is exposed on the outer surface and is readily available to trap free radicals, whereas a second co-antioxidant (like quercetin) is loaded in the inner lumen and is slowly released to regenerate the main antioxidant and afford a prolonged synergistic protection (Fig. 17b).

Co-delivery of two or more biological active compounds has attracted increasing attention because it is known that compared to conventional single-agent treatment, multi-agent therapy can promote the synergism of different drugs, increase therapeutic target selectivity, and overcome drug resistance through distinct mechanisms of action.

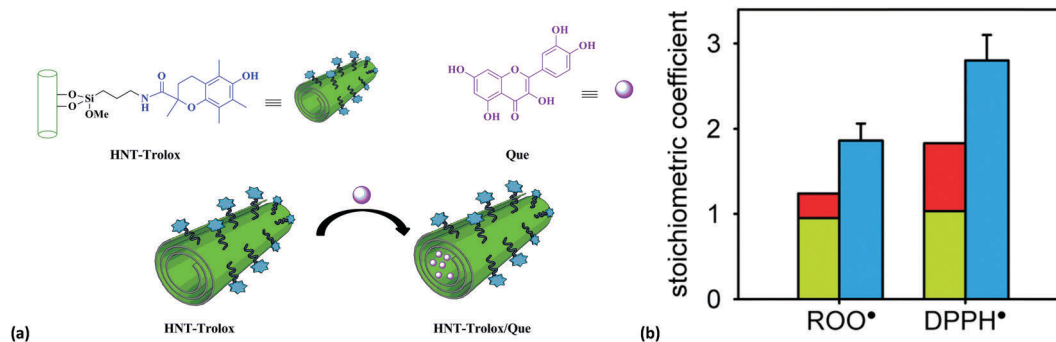


Fig. 17 (a) Schematic representation of quercetin loading into HNT-Trolox. (b) Synergistic effect in HNT-Trolox/Que: the experimental stoichiometric coefficient in MeCN (blue bars, \pm SD, $N = 3$) compared to the theoretical one, as calculated from the sum of contributions of HNT-Trolox (green bars) and HNT/Que (red bars) alone.

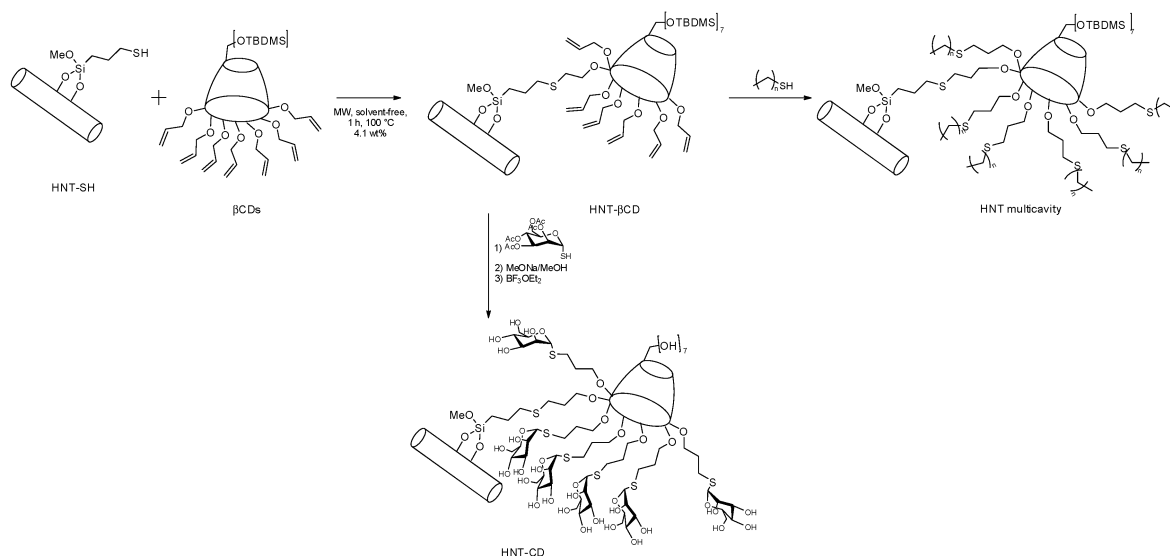
Recently Zhou *et al.* reported a dual-drug delivery system comprising poly(L-lactide) (PLLA)/HNT electrospun mats capable of co-delivering hydrophilic (polymyxin B) and hydrophobic (dexamethasone) drugs.⁸⁰ Filling of electrospun PLLA mats with HNTs shows that the nanocomposite obtained presents an increase in the breaking stress and, in addition, the mats degraded more rapidly when compared to pure electrospun mats, under the same conditions. Moreover, the presence of HNTs in the fibers facilitated the tunable release of polymyxin B and dexamethasone. The composite fiber mats exhibited considerable antibacterial activity and put forward the use of halloysite as wound-dressing materials.

Another dual-drug HNT delivery system was obtained by the covalent linkage of β -cyclodextrin (β -CD) units on the HNT external surface.⁶⁴ The covalent binding of cyclodextrin instead of a supramolecular approach to the HNT surface allows the fabrication of an organic-inorganic hybrid material with great stability, control over the degree of functionalization, and the data reproducibility. Moreover, the presence of two cavities offers the remarkable possibility for a simultaneous encapsulation of

two or more drug molecules with different physicochemical properties, followed by a different path release in agreement with the cavity that encapsulates each drug. In this context, different systems were developed (Scheme 4).

One of them was obtained by grafting amphiphilic cyclodextrin units onto the nanotube surface and the new multicavity nanomaterial was used for the simultaneous co-delivery of silibinin and quercetin.²⁶ HPLC measurements and fluorescence spectroscopy highlighted that silibinin interacts preferentially with the HNT lumen, while quercetin does with the cyclodextrin cavity. Thermogravimetric analysis showed that the new materials can load the drugs and, therefore, they are suitable nanocontainers for the co-delivery of two drugs that could have synergistic effects in anticancer therapy as demonstrated by *in vitro* cytotoxicity assays. In addition, the interaction between cells and the carrier, analyzed by fluorescence microscopy, revealed that the materials were taken up into cells surrounding the nuclei (Fig. 18).

Since drug delivery to specific targets has become an important issue for promoting the selectivity of drugs to diseased



Scheme 4 Schematic representation of the synthesis of the HNT multicavity and HNT-CD.

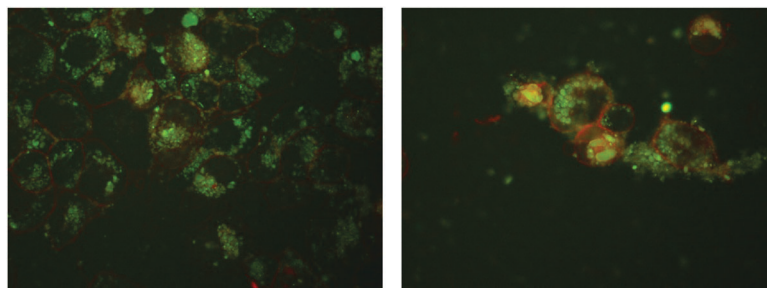


Fig. 18 Fluorescence microscopy images of the HNT multicavity uptake by 8505C. An 8505C cell membrane (red) with a co-localized HNT multicavity (green) surrounding cell nuclei at 24 h.

sites and reducing toxicity against normal cells, the introduction of targeting functionalities as well as the glycocluster effect on halloysite systems was achieved by attaching on several β -CD core mannose units (Scheme 4).²⁷ Also in this case, the novel nanomaterial was employed for the co-delivery of curcumin and silibinin. Release studies showed that pH deeply affects the kinetic course of the process, and at different pH values, indeed, a complementary behavior of drugs was observed. In particular, curcumin showed a slow release in the simulated gastric fluid, whereas a more rapid release rate was observed in the simulated intestinal fluid. In contrast, silibinin was better released in an acidic environment (Fig. 19). This complementary behavior, mainly due to the different “interaction sites” on the HNT-CD system could be advantageous for the actual application to maintain effective concentration in the body and reduce the maximum extent of the side effects to the stomach.

In order to better understand the release behavior of silibinin and curcumin under different pH conditions, the *in vitro* release data were fitted to two models to analyze the kinetics and the release mechanism of both molecules. The experimental data were analyzed using (DEM) and Korsmeyer–Peppas models. The results showed that the release of silibinin at pH 1.0 and curcumin at both pH values follows the Korsmeyer–Peppas model with an n value lower than 0.5 in all cases, indicating that the release of biological molecules was controlled by a drug diffusion process. It was found that the release

mode of silibinin in neutral solution follows the double exponential model. Therefore, the release of silibinin and the simultaneous release of curcumin were observed. The dual-drug loaded system showed an improved cytotoxic activity against 8505C cell lines compared to free drugs. The associated activity might be attributed to the enhanced cellular internalization due to carbohydrate-receptor-mediated endocytosis with nuclear specific targeting as highlighted by fluorescence microscopy. This result demonstrates that halloysite could penetrate the cellular membrane and surrounding cell nuclei.²⁷

6 Functionalized halloysite nanotubes and biopolymers for biological applications

Biopolymers are usually used for controlled drug delivery. However, pristine biopolymer matrices suffer from some disadvantages such as the burst release of drugs and weak stability. Besides the improved mechanical properties,¹⁹ inorganic materials have been used to improve the swelling behavior, drug loading efficiency and controlled release behavior of the pristine biopolymer matrices *via* electrostatic interactions and hydrogen bonding. Therefore, the combination of HNTs and biopolymers should be a feasible approach to prepare carriers for sustained drug release.⁸¹

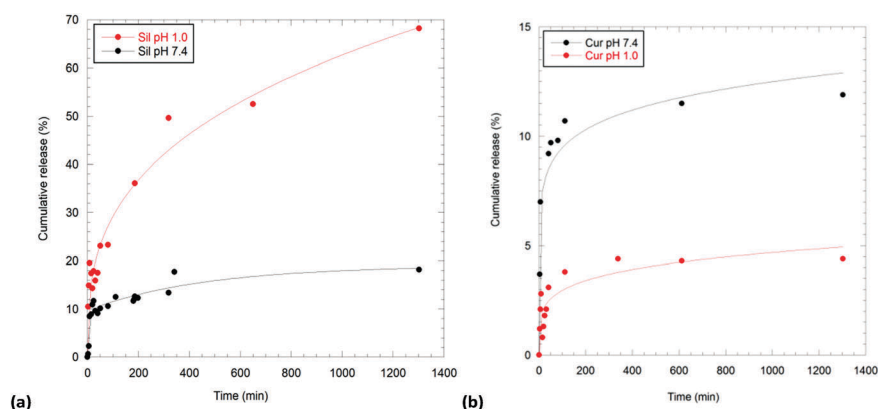


Fig. 19 Kinetic release of (a) silibinin; (b) curcumin in 0.1 M HCl solution and pH 7.4 phosphate buffer from HNT-CD hybrids.

Fan *et al.*⁸² reported the preparation of HNT-sodium alginate/hydroxyapatite nanocomposite beads by the generation of hydroxyapatite (HA) in a nanosized regime. To this aim the sol-gel transition of the HNT-sodium alginate dispersion was used to produce the nanoparticles *in situ*. The beads were used for the loading and release of diclofenac sodium. The combination of HNTs with a tubular structure and HA nanoparticles could limit the flexibility of the alginate polymer chains, which is the principal reason for the enhanced loading of the active pharmaceutical component. Moreover, a sustained release behavior is achieved.

Magnetic microspheres, 2-hydroxypropyltrimethyl ammonium chloride chitosan/ Fe_3O_4 /halloysite nanotubes/ofloxacin (HACC/ Fe_3O_4 /HNTs/OFL), for the controlled release of OFL were synthesized by *in situ* crosslinking with glutaraldehyde in the spray-drying process (Fig. 20). The magnetic microspheres were employed as carriers for ofloxacin. It was found that HNTs have a remarkable effect on the roughness of the surface, which decreases the entrapment efficiency and accelerates the release of OFL though an increase in HNT content, and are conducive to the adsorption of OFL into HNTs.

However, the introduction of HNTs can improve the bio-availability of OFL in the gastro-retentive drug delivery system.⁸³

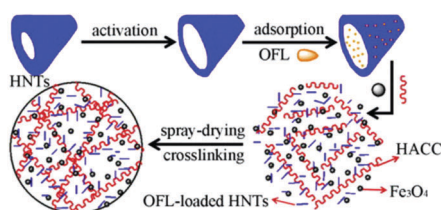


Fig. 20 Preparation of the hydroxypropyltrimethyl ammonium chloride chitosan/ Fe_3O_4 /halloysite nanotubes/ofloxacin (HACC/ Fe_3O_4 /HNTs/OFL) microsphere. Reproduced from ref. 83 with permission from Elsevier.

Due to its features, among them hemostatic and anti-infectious activities, chitosan can also be used for wound healing. Chitosan can accelerate the infiltration of polymorphonuclear cells at the early stage of wound healing, followed by the fabrication of collagen by fibroblasts.

The addition of HNTs aids in faster re-epithelialization and collagen deposition. These properties are attributed to the particular characteristics of HNTs and their combination with chitosan. The results show that these advanced HNT-chitosan bionanocomposite sponges have many potential applications for diabetic, burn and chronic wound infections.⁸⁴

Thanks to the high performance and biocompatibility, HNT-chitosan and HNT-alginate bionanocomposites also have possible applications in bone tissue engineering. In order to verify cell attachment and viability on the bionanocomposites, several studies were carried out. Cell morphology results exhibited that cells can be attached and grown well on the chitosan-HNTs.^{6,85} The introduction of HNTs caused changes in the surface topography of chitosan and involved an increasing roughness of the bionanocomposite. A rougher surface and the existence of the Si element in the HNTs-chitosan bionanocomposite surface are beneficial to the attachment of the cells.

Bionanocomposite films based on chitosan reinforced with HNT were able to trap horseradish peroxidase (HRP). Besides its use as a immobilization matrix, chitosan/HNT was proposed as a binder to improve the adhesive features to an electrode surface. In particular, the obtained HNT-chitosan film could promote the direct electrochemistry of HRP and catalyze the reduction of H_2O_2 .⁸⁶ Therefore, this hydrophilic HNTs-chitosan bionanocomposite could give a new appealing platform for additional studies on the redox behavior of proteins. The use of a direct electrochemistry approach is crucial for the development of innovative biosensors.

Gorrasi *et al.*⁸⁷ reported the synthesis and characterization of bionanocomposites based on pectins and nano-hybrids of

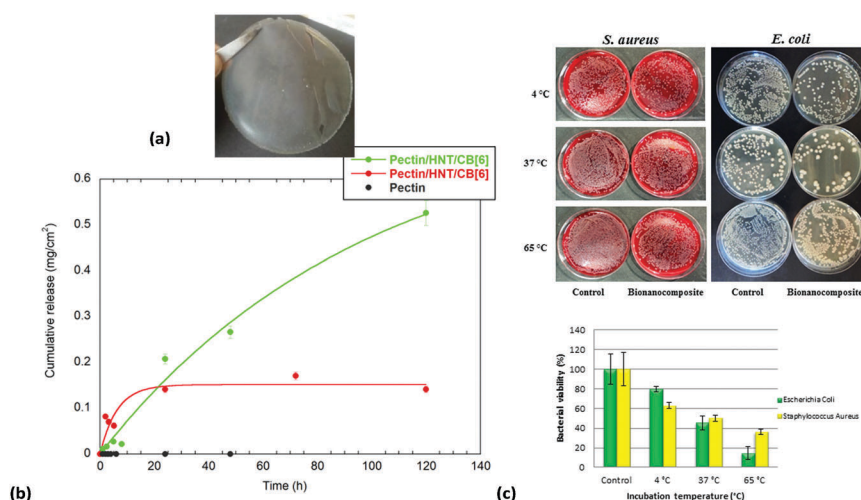


Fig. 21 (a) Pectin/HNT/CB[6]/peppermint oil bionanocomposite film. (b) Release profile of menthone (expressed as mg of menthone per cm^2 of film) from the pectin based films in 50% v/v ethanol. Black circles refer to pristine pectin at 25 °C, while green and red circles refer to the pectin/HNT/CB[6] bionanocomposite at 4 and 25 °C, respectively. (c) Antibacterial activity of pectin/HNT/PO films against *E. coli* and *S. aureus* at 4, 37 and 65 °C incubated for 30 min.⁸⁸

HNTs loaded with rosemary essential oil, as antimicrobial agents, for their potential application in food packaging. The halloysite presents improved mechanical and barrier properties, allowing a much slower release of rosmarinic acid compared to the molecules directly dispersed in the pectins and a preliminary evaluation of antimicrobial activity indicated the potential application of the obtained composites in active food packaging, opening new aspects for pectins-antimicrobials as coating agents for their application in the food packaging field.

The loading of essential peppermint oil in a novel edible biodegradable film based on pectin reinforced with functionalized HNT was also reported (Fig. 21).⁸⁸ In particular, supramolecular interactions between HNT surfaces and cucurbit[6]uril (CB[6]) molecules⁸⁹ facilitated the synthesis of a hybrid nanofiller with high solubilization capacity towards essential oils.

The “multi-pocket” HNT/CB[6] filler showed a significant enhancement (*ca.* 10 times) of the HNT adsorption ability towards peppermint oil, which was induced by the addition of CB[6], as confirmed by HPLC analysis. On this basis, HNT/CB[6] loaded with the essential oil was filled in a pectin matrix using the aqueous casting method under vacuum as well as a peppermint oil saturated atmosphere. With the ultimate goal of using this bionanocomposite for food packaging applications, some release tests were performed in the simulant food solvent. These results showed that the bionanocomposite could be considered as a thermo-sensitive packaging system. With respect to antimicrobial properties, *in vitro* experiments for *Escherichia coli* (Gram-negative) and *Staphylococcus aureus* (Gram-positive) isolated from food sources revealed that the composite biofilm is more efficient at higher temperatures (Fig. 21c).

7 Conclusions and perspectives

Halloysite nanotubes are made of natural aluminosilicate clay with a hollow tubular structure in the sub-micrometer range and dimensions suitable for macrophage removal from living cells. They are classified as class 4 materials (low hazard substances). HNTs contain siloxane groups on the external surface, whereas aluminol groups are present in the inner lumen. The possibility of modifying both surfaces *via* both chemical and supramolecular interactions opens up a lot of ways to use these interesting nanomaterials in several fields, especially in drug transport and delivery. The introduction of specific groups to HNT surfaces is an important task since it enables synergy between drugs with different physicochemical and biological properties as well as a different path release. Furthermore, it is possible to affect a triggered release based on an external stimulus. Finally, the presence of target moieties allows the cellular uptake of the nanomaterial and in the same cases, it is demonstrated that the carrier can overcome the cellular barrier, even penetrating into cell nuclei. Several biological tests highlight that halloysite is a safe material and therefore it is promising for specific applications for the treatment of several diseases. In the light of the fact that halloysite is used as a non-injectable drug formulation, interest in its use as a drug carrier and delivery system depends on its incorporation into oral tablets, sprays, creams and so on.

Acknowledgements

The authors are thankful to Dr Julie Perkins. This work was financially supported by the University of Palermo (Italy), FIRB 2012 (prot. RBFR12ETL5) and PON-TECLA (PON03PE_00214_1).

Notes and references

- 1 P. Bethier, *Ann. Chim. Phys.*, 1826, **32**, 332–335.
- 2 B. P. Gaber, Y. Lvov and R. R. Price, *J. Microencapsulation*, 2001, **18**, 713–722.
- 3 S. J. Antill, *Aust. J. Chem.*, 2003, **56**, 723.
- 4 M. Kryuchkova, A. Danilushkina, Y. Lvov and R. Fakhrullin, *Environ. Sci.: Nano*, 2016, **3**, 442–452.
- 5 M. Liu, R. He, J. Yang, W. Zhao and C. Zhou, *ACS Appl. Mater. Interfaces*, 2016, **8**, 7709–7719.
- 6 M. Liu, C. Wu, Y. Jiao, S. Xiong and C. Zhou, *J. Mater. Chem. B*, 2013, **1**, 2078–2089.
- 7 G. I. Fakhrullina, F. S. Akhatova, Y. M. Lvov and R. F. Fakhrullin, *Environ. Sci.: Nano*, 2015, **2**, 54–59.
- 8 E. A. Naumenko, I. D. Guryanov, R. Yendluri, Y. M. Lvov and R. F. Fakhrullin, *Nanoscale*, 2016, **8**, 7257–7271.
- 9 L. Bellani, L. Giorgetti, S. Riela, G. Lazzara, A. Scialabba and M. Massaro, *Environ. Toxicol. Chem.*, 2016, **35**, 2503–2510.
- 10 A. D. Hughes and M. R. King, *Langmuir*, 2010, **26**, 12155–12164.
- 11 A. D. Hughes, G. Marsh, R. E. Waugh, D. G. Foster and M. R. King, *Langmuir*, 2015, **31**, 13553–13560.
- 12 E. Abdullayev and Y. Lvov, *J. Mater. Chem. B*, 2013, **1**, 2894–2903.
- 13 G. Jock Churchman, P. Pasbakhsh, D. J. Lowe and B. K. G. Theng, *Clay Miner.*, 2016, **51**, 395–416.
- 14 L. Guimarães, A. N. Enyashin, G. Seifert and H. A. Duarte, *J. Phys. Chem. C*, 2010, **114**, 11358–11363.
- 15 F. Ferrante, N. Armata and G. Lazzara, *J. Phys. Chem. C*, 2015, **119**, 16700–16707.
- 16 Y. Lvov and E. Abdullayev, *Prog. Polym. Sci.*, 2013, **38**, 1690–1719.
- 17 E. Abdullayev, V. Abbasov, A. Tursunbayeva, V. Portnov, H. Ibrahimov, G. Mukhtarova and Y. Lvov, *ACS Appl. Mater. Interfaces*, 2013, **5**, 4464–4471.
- 18 W. O. Yah, A. Takahara and Y. M. Lvov, *J. Am. Chem. Soc.*, 2012, **134**, 1853–1859.
- 19 F. Arcudi, G. Cavallaro, G. Lazzara, M. Massaro, S. Milioto, R. Noto and S. Riela, *J. Phys. Chem. C*, 2014, **118**, 15095–15101.
- 20 M. Massaro, V. Schembri, V. Campisciano, G. Cavallaro, G. Lazzara, S. Milioto, R. Noto, F. Parisi and S. Riela, *RSC Adv.*, 2016, **6**, 55312–55318.
- 21 M. Massaro, S. Riela, G. Cavallaro, C. G. Colletti, S. Milioto, R. Noto, F. Parisi and G. Lazzara, *J. Mol. Catal. A: Chem.*, 2015, **408**, 12–19.
- 22 N. G. Veerabadran, R. R. Price and Y. M. Lvov, *Nano*, 2007, **02**, 115–120.
- 23 C. Bretti, S. Cataldo, A. Gianguzza, G. Lando, G. Lazzara, A. Pettignano and S. Sammartano, *J. Phys. Chem. C*, 2016, **120**, 7849–7859.

- 24 Y. Lvov, W. Wang, L. Zhang and R. Fakhrullin, *Adv. Mater.*, 2016, **28**, 1227–1250.
- 25 S. Riela, M. Massaro, C. G. Colletti, A. Bommarito, C. Giordano, S. Milioto, R. Noto, P. Poma and G. Lazzara, *Int. J. Pharm.*, 2014, **475**, 613–623.
- 26 M. Massaro, S. Piana, C. G. Colletti, R. Noto, S. Riela, C. Baiamonte, C. Giordano, G. Pizzolanti, G. Cavallaro, S. Milioto and G. Lazzara, *J. Mater. Chem. B*, 2015, **3**, 4074–4081.
- 27 M. Massaro, S. Riela, C. Baiamonte, J. L. J. Blanco, C. Giordano, P. Lo Meo, S. Milioto, R. Noto, F. Parisi, G. Pizzolanti and G. Lazzara, *RSC Adv.*, 2016, **6**, 87935–87944.
- 28 M. Massaro, R. Amorati, G. Cavallaro, S. Guernelli, G. Lazzara, S. Milioto, R. Noto, P. Poma and S. Riela, *Colloids Surf., B*, 2016, **140**, 505–513.
- 29 M. Massaro, C. G. Colletti, R. Noto, S. Riela, P. Poma, S. Guernelli, F. Parisi, S. Milioto and G. Lazzara, *Int. J. Pharm.*, 2015, **478**, 476–485.
- 30 D. S. Kommireddy, S. M. Sriram, Y. M. Lvov and D. K. Mills, *Biomaterials*, 2006, **27**, 4296–4303.
- 31 Y. Lvov, A. Aerov and R. Fakhrullin, *Adv. Colloid Interface Sci.*, 2014, **207**, 189–198.
- 32 Y. Zhang, Y. Chen, H. Zhang, B. Zhang and J. Liu, *J. Inorg. Biochem.*, 2013, **118**, 59–64.
- 33 S. A. Konnova, I. R. Sharipova, T. A. Demina, Y. N. Osin, D. R. Yarullina, O. N. Ilinskaya, Y. M. Lvov and R. F. Fakhrullin, *Chem. Commun.*, 2013, **49**, 4208–4210.
- 34 F. R. Ahmed, M. H. Shoaib, M. Azhar, S. H. Um, R. I. Yousuf, S. Hashmi and A. Dar, *Colloids Surf., B*, 2015, **135**, 50–55.
- 35 Y. M. Lvov, M. M. DeVilliers and R. F. Fakhrullin, *Expert Opin. Drug Delivery*, 2016, **13**, 977–986.
- 36 N. M. Mitrokhin, M. L. Gowbeva, I. N. Razumnaya, S. D. Fastov and I. S. Fatov, *Toksikol. Vestn.*, 2016, **2**, 52–55.
- 37 P. Yuan, P. D. Southon, Z. Liu, M. E. R. Green, J. M. Hook, S. J. Antill and C. J. Kepert, *J. Phys. Chem. C*, 2008, **112**, 15742–15751.
- 38 S. Wu, M. Qiu, B. Guo, L. Zhang and Y. M. Lvov, *ACS Sustainable Chem. Eng.*, 2017, **5**, 1775–1783.
- 39 J. Tully, R. Yendluri and Y. Lvov, *Biomacromolecules*, 2016, **17**, 615–621.
- 40 M. R. Dзамukova, E. A. Naumenko, Y. M. Lvov and R. F. Fakhrullin, *Sci. Rep.*, 2015, **5**, 10560.
- 41 C. Aguzzi, P. Cerezo, C. Viseras and C. Caramella, *Appl. Clay Sci.*, 2007, **36**, 22–36.
- 42 D. Tan, P. Yuan, F. Annabi-Bergaya, D. Liu, L. Wang, H. Liu and H. He, *Appl. Clay Sci.*, 2014, **96**, 50–55.
- 43 J. Huang, Z. Tang and B. Guo, *RSC Smart Materials*, 2017, pp. 157–186.
- 44 P. Pasbakhsh, H. Ismail, M. N. A. Fauzi and A. A. Bakar, *Appl. Clay Sci.*, 2010, **48**, 405–413.
- 45 M. Liu, Y. Chang, J. Yang, Y. You, R. He, T. Chen and C. Zhou, *J. Mater. Chem. B*, 2016, **4**, 2253–2263.
- 46 S. S. Zargarian, V. Haddadi-Asl and H. Hematpour, *J. Nanopart. Res.*, 2015, **17**, 1–13.
- 47 Y. Joo, Y. Jeon, S. U. Lee, J. H. Sim, J. Ryu, S. Lee, H. Lee and D. Sohn, *J. Phys. Chem. C*, 2012, **116**, 18230–18235.
- 48 F. Shahamati Fard, S. Akbari, E. Pajootan and M. Arami, *Desalin. Water Treat.*, 2016, **57**, 26222–26239.
- 49 X. Tian, W. Wang, Y. Wang, S. Komarneni and C. Yang, *Microporous Mesoporous Mater.*, 2015, **207**, 46–52.
- 50 G. Cavallaro, G. Lazzara, M. Massaro, S. Milioto, R. Noto, F. Parisi and S. Riela, *J. Phys. Chem. C*, 2015, **119**, 8944–8951.
- 51 M. Liu, B. Guo, M. Du, Y. Lei and D. Jia, *J. Polym. Res.*, 2008, **15**, 205–212.
- 52 Y. Hou, J. Jiang, K. Li, Y. Zhang and J. Liu, *J. Phys. Chem. B*, 2014, **118**, 1962–1967.
- 53 M. T. Albdiry and B. F. Yousif, *Mater. Des.*, 2013, **48**, 68–76.
- 54 A. F. Peixoto, A. C. Fernandes, C. Pereira, J. Pires and C. Freire, *Microporous Mesoporous Mater.*, 2016, **219**, 145–154.
- 55 X. T. Cao, A. M. Showkat, D. W. Kim, Y. T. Jeong, J. S. Kim and K. T. Lim, *J. Nanosci. Nanotechnol.*, 2015, **15**, 8617–8621.
- 56 H. Li, X. Zhu, H. Zhou and S. Zhong, *Colloids Surf., A*, 2015, **487**, 154–161.
- 57 H. Lun, J. Ouyang and H. Yang, *RSC Adv.*, 2014, **4**, 44197–44202.
- 58 C. Li, J. Liu, X. Qu, B. Guo and Z. Yang, *J. Appl. Polym. Sci.*, 2008, **110**, 3638–3646.
- 59 C. Li, J. Liu, X. Qu and Z. Yang, *J. Appl. Polym. Sci.*, 2009, **112**, 2647–2655.
- 60 J. Zhang, D. Zhang, A. Zhang, Z. Jia and D. Jia, *Iran. Polym. J.*, 2013, **22**, 501–510.
- 61 E. Bischoff, T. Daitx, D. A. Simon, H. S. Schrekker, S. A. Liberman and R. S. Mauler, *Appl. Clay Sci.*, 2015, **112–113**, 68–74.
- 62 L. N. Carli, T. S. Daitx, G. V. Soares, J. S. Crespo and R. S. Mauler, *Appl. Clay Sci.*, 2014, **87**, 311–319.
- 63 M. Massaro, S. Riela, G. Lazzara, M. Gruttadauria, S. Milioto and R. Noto, *Appl. Organomet. Chem.*, 2014, **28**, 234–238.
- 64 M. Massaro, S. Riela, P. Lo Meo, R. Noto, G. Cavallaro, S. Milioto and G. Lazzara, *J. Mater. Chem. B*, 2014, **2**, 7732–7738.
- 65 P. Luo, J.-S. Zhang, B. Zhang, J.-H. Wang, Y.-F. Zhao and J.-D. Liu, *Ind. Eng. Chem. Res.*, 2011, **50**, 10246–10252.
- 66 S. Barrientos-Ramirez, G. M. de Oca-Ramirez, E. V. Ramos-Fernandez, A. Sepulveda-Escribano, M. M. Pastor-Blas and A. Gonzalez-Montiel, *Appl. Catal., A*, 2011, **406**, 22–33.
- 67 B. Guo, Q. Zou, Y. Lei and D. Jia, *Polym. J.*, 2009, **41**, 835–842.
- 68 J. Zhang, D. Zhang, A. Zhang, Z. Jia and D. Jia, *J. Reinf. Plast. Compos.*, 2013, **32**, 713–725.
- 69 V. S. Raman, S. Rooj, A. Das, K. W. Stöckelhuber, F. Simon, G. B. Nando and G. Heinrich, *J. Macromol. Sci., Part A: Pure Appl. Chem.*, 2013, **50**, 1091–1106.
- 70 N. G. Veerabadran, D. Mongayt, V. Torchilin, R. R. Price and Y. M. Lvov, *Macromol. Rapid Commun.*, 2009, **30**, 99–103.
- 71 D. Tan, P. Yuan, F. Annabi-Bergaya, H. Yu, D. Liu, H. Liu and H. He, *Microporous Mesoporous Mater.*, 2013, **179**, 89–98.
- 72 S. Kumar-Krishnan, A. Hernandez-Rangel, U. Pal, O. Ceballos-Sanchez, F. J. Flores-Ruiz, E. Prokhorov, O. Arias de Fuentes, R. Esparza and M. Meyyappan, *J. Mater. Chem. B*, 2016, **4**, 2553–2560.
- 73 J. M. Goran, S. M. Mantilla and K. J. Stevenson, *Anal. Chem.*, 2013, **85**, 1571–1581.

- 74 J. Yang, Y. Wu, Y. Shen, C. Zhou, Y.-F. Li, R.-R. He and M. Liu, *ACS Appl. Mater. Interfaces*, 2016, **8**, 26578–26590.
- 75 G. Cavallaro, G. Lazzara and S. Milioto, *Langmuir*, 2011, **27**, 1158–1167.
- 76 R. Noël, X. Song, R. Jiang, M. J. Chalmers, P. R. Griffin and T. M. Kamenecka, *J. Org. Chem.*, 2009, **74**, 7595–7597.
- 77 H. Hemmatpour, V. Haddadi-Asl and H. Roghani-Mamaqani, *Polymer*, 2015, **65**, 143–153.
- 78 M. Du, B. Guo and D. Jia, *Eur. Polym. J.*, 2006, **42**, 1362–1369.
- 79 M. Massaro, S. Riela, S. Guernelli, F. Parisi, G. Lazzara, A. Baschieri, L. Valgimigli and R. Amorati, *J. Mater. Chem. B*, 2016, **4**, 2229–2241.
- 80 X. Zhang, R. Guo, J. Xu, Y. Lan, Y. Jiao, C. Zhou and Y. Zhao, *J. Biomater. Appl.*, 2015, **30**, 512–525.
- 81 P. Pasbakhsh, G. J. Churchman and J. L. Keeling, *Appl. Clay Sci.*, 2013, **74**, 47–57.
- 82 L. Fan, J. Zhang and A. Wang, *J. Mater. Chem. B*, 2013, **1**, 6261–6270.
- 83 Q. Wang, J. Zhang, B. Mu, L. Fan and A. Wang, *Carbohydr. Polym.*, 2014, **102**, 877–883.
- 84 M. Liu, Y. Shen, P. Ao, L. Dai, Z. Liu and C. Zhou, *RSC Adv.*, 2014, **4**, 23540–23553.
- 85 M. Liu, Y. Zhang, C. Wu, S. Xiong and C. Zhou, *Int. J. Biol. Macromol.*, 2012, **51**, 566–575.
- 86 X. Sun, Y. Zhang, H. Shen and N. Jia, *Electrochim. Acta*, 2010, **56**, 700–705.
- 87 G. Gorrasi, *Carbohydr. Polym.*, 2015, **127**, 47–53.
- 88 G. Biddeci, G. Cavallaro, F. Di Blasi, G. Lazzara, M. Massaro, S. Milioto, F. Parisi, S. Riela and G. Spinelli, *Carbohydr. Polym.*, 2016, **152**, 548–557.
- 89 M. Massaro, S. Riela, G. Cavallaro, C. G. Colletti, S. Milioto, R. Noto and G. Lazzara, *ChemistrySelect*, 2016, **1**, 1773–1779.